www.amlett.com, www.amlett.org, DOI: 10.5185/amlett.2012.ib.111
"Nanostructuring by electrons, photons and ions" Special Issue Published online by the VBRI press in 2013

In-situ TEM observation of electron irradiation induced shape transition of elongated gold nanoparticles embedded in silica

S. Mohapatra[1*], Y.K. Mishra[2], J. Ghatak[3], D.K. Avasthi[4]

[1]*School of Basic and Applied Sciences, Guru Gobind Singh Indraprastha University, Dwarka, New Delhi 110075, India*
[2]*Functional Nanomaterials, Institute for Materials Science, University of Kiel, Kaiserstrasse 2, 24143 Kiel, Germany*
[3]*Department of Material Science and Engineering, University of Sheffield, Sheffield, South Yorkshire, UK*
[4]*Inter University Accelerator Centre, Post Box -10502, New Delhi 110067, India*

[*]Corresponding author. Tel. (+91) 11 25302414; E-mail: smiuac@gmail.com

Received: 16 March 2012, Revised: 22 July 2012 and Accepted: 26 July 2012

ABSTRACT

Elongated Au nanoparticles (NPs) embedded in silica matrix were fabricated by 100 MeV Ag ion irradiation of 3 MeV Au ion implanted SiO_2/Si(100) substrates, annealed at 1050^{o}C. Electron-beam-induced shape evolution of elongated Au NPs embedded in SiO_2 has been studied by high resolution transmission electron microscopy. Electron beam irradiation resulted in a decrease in the aspect ratio of Au NPs from ~ 1.4 to 1 with increase in irradiation time. The observed ellipsoidal-to-spherical shape transition of Au NPs has been ascribed mainly to the cumulative effects of electron beam induced heating, softening of silica matrix and radiation enhanced diffusion of knock-on displaced O and Si atoms, resulting in local stress relaxation. Copyright © 2013 VBRI press.

Keywords: Gold nanoparticles; electron beam; transmission electron microscopy.

Satyabrata Mohapatra is working as Assistant Professor of Nanoscience and Technology at School of Basic and Applied Sciences, Guru Gobind Singh Indraprastha University, New Delhi, India. He obtained his Ph. D. in Physics in 2006 from Institute of Physics (IOP), Bhubaneswar. He has worked as Postdoctoral Research Fellow at Materials Science Group, Inter University Accelerator Centre, New Delhi. His current research mainly involves synthesis and ion beam engineering of functional nanostructures and plasmonic nanocomposites for optical and biomedical applications.

Yogendra Mishra is working Alexander von Humboldt Fellow at Functional Nanomaterials, in Institute of Materials Science, University of Kiel, Kiel Germany. He obtained Master in 2003 from University of Allahabad, Allahabad, and Ph. D. in Physics in 2008 in Physics from Inter University Accelerator Centre-Jawaharlal Nehru University, New Delhi. India. His current research mainly involves synthesis of metal semiconductor nanostructures and their electrical and biomedical applications.

Devesh Kumar Avasthi is Group Leader for materials science and radiation biology at Inter University Accelerator Centre, New Delhi. He implemented elastic recoil detection analysis (ERDA) technique for light element depth profiling. Later a gaseous telescope detector was designed, fabricated and installed to enhance the capabilities of ERDA, which was used for electronic sputtering measurements. The facilities for thin film development and vacuum laboratory were developed to take care of need of accelerator. The most recent developments of his group have been an atom beam sputtering set up for synthesis of nanocomposite thin films, in-situ ERDA, in-situ XRD, in-situ QMA in beam line. His main interest is ion beams for analysis, modification of materials, synthesis and engineering the nanostructures by ion beams. Currently his interest has been creation and modification of nanostructures by ion beams. He had major research projects under 'Intensifying Research in High Priority Area' scheme and currently a project under 'Nano Mission' funded by Department of Science and Technology, Government of India. Dr.Avasthi had several international collaborations with research groups in Munich, Stuttgart, Kiel, Orsay and Padova. He is a member of international committee for the conferences on 'Ion Beam Analysis' and 'Swift Heavy Ion in Matter'. He has several conference proceedings as editor and more than three hundred research papers to his credit.

Introduction

Metal nanostructures embedded in dielectric matrix exhibit unique physical and chemical properties, widely different from that of bulk. The size and shape dependent properties of metal nanostructures make them promising for a wide range of applications in nanoelectronics, photonics, telecommunications and bio-medical engineering [**1-7**]. Several physical and chemical methods have been employed for the synthesis of metal nanostructures embedded in various dielectric matrices [**8-14**]. For their applications in nanotechnology, it is very important to controllably tailor the size and shape of metal nanostructures. Irradiation with energetic ion beams has emerged a unique tool to tailor the shape and size distribution of embedded metal nanoparticles (NPs) [**15-20**]. Recent studies have shown that electron beam irradiation can also be used for tailoring the size distribution of metal NPs in nanocomposites [**21-26**]. The effects of electron beam irradiation on the shape and size distribution of embedded NPs is of interest since during TEM measurements the nanocomposites are exposed to energetic electrons. In a recent study [**26**], we have shown that 200 keV electron beam irradiation of Au-silica nanocomposites leads to controlled growth of Au NPs. However, electron beam irradiation induced shape change of Au NPs have not been reported so far to the best of our knowledge. Electron beam irradiation can cause quasi-melting of small nanoclusters and also result in relaxation of strain in embedded nanostructures leading to their shape change. In this letter, we report an *in-situ* TEM investigation of electron-beam-induced shape evolution of elongated Au NPs embedded in SiO_2 and analyze the mechanisms underlying the shape change. We demonstrate that electron beam irradiation can be used as an effective tool to tailor the shape of Au NPs embedded in SiO_2.

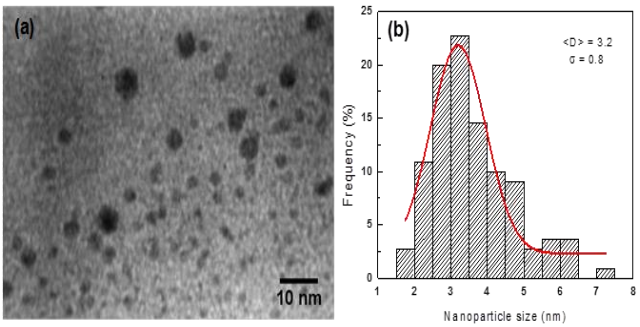

Fig. 1. (a) Cross sectional TEM image of the as-annealed sample. (b) size distribution of Au NPs embedded in SiO_2 film.

Experimental

Amorphous SiO_2 thin films with thickness ~950 nm were grown on Si(100) substrates by wet thermal oxidation. Nanometer-sized Au particles (average size 2 nm) embedded in SiO_2 were synthesized by 3 MeV Au^{3+} ion implantation to a fluence of 6 x 10^{15} ions cm^{-2} followed by annealing in air at 1050°C. Annealed samples were then irradiated with 100 MeV Ag ions to a fluence of 1 x 10^{14} ions cm^{-2} using 15UD Pelletron accelerator facility at IUAC, New Delhi. The microstructure of the annealed and irradiated sample was studied by cross sectional TEM at 200 keV using JEOL 2010 UHR TEM facility at Institute of Physics, Bhubaneswar. *In-situ* TEM experiments were carried out at 200 keV for investigating the electron-beam-induced shape evolution of Au NPs embedded in SiO_2 film in the irradiated sample. HRTEM studies on Au NPs embedded in SiO_2 were carried out for studying the crystal structure, shape and size of Au NPs. HRTEM images of Au NPs were recorded after every 5 minutes of electron beam irradiation, at the same spot.

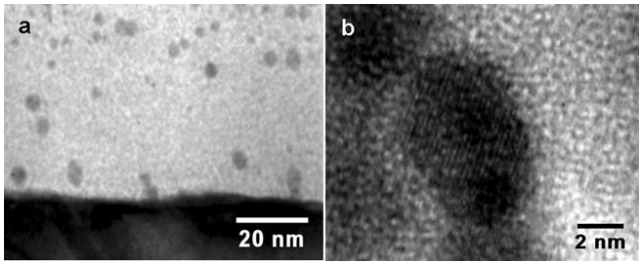

Fig. 2. (a) Cross sectional TEM image of the irradiated sample. (b) HRTEM image of one elongated Au NP embedded in SiO_2 film.

Results and discussion

Fig. 1 (a) shows bright field cross sectional TEM image of the annealed sample before irradiation, which reveals the presence of spherical Au NPs in embedded in SiO_2 layer. The size distribution of these Au NPs in the SiO_2 layer is shown in **Fig. 1**(b). The average size of these Au NPs has been found to be ~ 3.2 ± 0.8 nm. In **Fig. 2**(a) we show the bright field cross sectional TEM image of the annealed sample, irradiated with 100 MeV Ag ions to a fluence of 1 x 10^{14} ions cm^{-2}. The presence of spherical Au NPs with average size ~ 2 nm together with elongated Au NPs of larger size can be clearly seen. The elongation of Au NPs has been found to be along the ion beam direction. The HRTEM image of one such elongated Au NP is shown as inset in **Fig. 2**(b). The major axis length is 5.5 nm while the minor axis length is 4 nm. The average aspect ratio (ratio of major-to-minor axis length) of elongated Au NPs has been found to be ~ 1.4. The passage of 100 MeV Ag ions through SiO_2 film containing Au NPs deposits electronic energy (S_e) of ~11.1 keV/nm, estimated using stopping range of ions in matter (SRIM) program [**27**]. This results in the formation of latent tracks of diameter ~ 8 nm in the SiO_2 film [**28**]. Each individual ion impact leads to the formation of thermal spike of duration ~ 10^{-12} s which results in transient melting and viscous flow of silica [**29**]. Elongation of Au NPs embedded in silica matrix upon swift heavy ion irradiation has been reported [**17-20**] and explained in different ways. Roorda et al. [**16**] have explained the deformation of Au NPs along ion beam direction in ion irradiated Au-silica core-shell nanostructures as a consequence of in-plane mechanical stress on silica shell acting perpendicular to the ion beam [**30**]. This pressure exerted by silica shell on the radiation softened Au core results in spherical-to-oblate shape transformation of Au NPs along ion beam direction. The second explanation is based on the fact that volume

expansion of Au while transforming from solid to molten state is more than that of silica undergoing similar transformation [**20**]. This leads to elongation of Au NPs along ion track in which small Au NPs and silica both exist in transiently molten state during thermal spike.

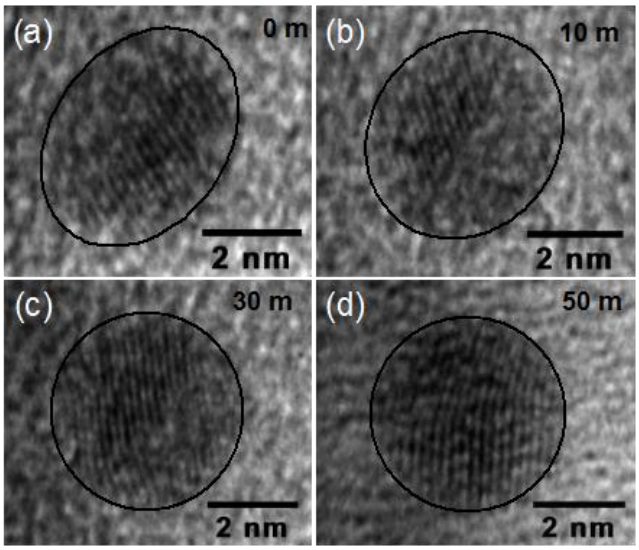

Fig. 3. HRTEM micrographs (a)-(d) showing a typical shape evolution of elongated Au NP embedded in SiO_2 during 200 keV electron beam irradiation. The numbers marked in each micrograph indicate the irradiation time in minutes.

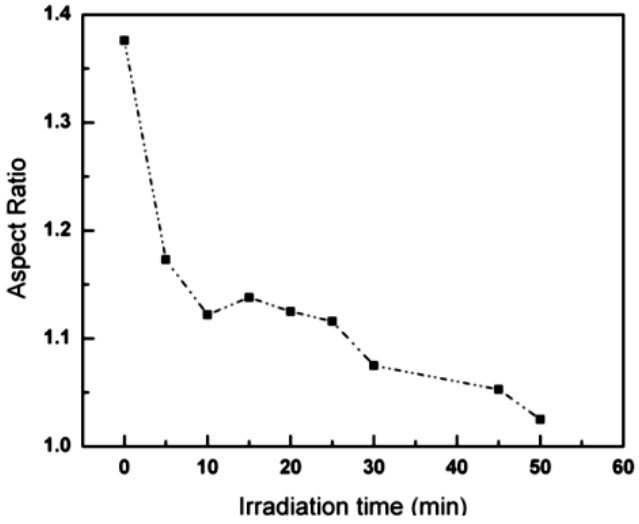

Fig. 4. Variation of aspect ratio of Au NP with electron beam irradiation time. The aspect ratio of Au NP was found to decrease from about 1.4 to 1 during electron beam irradiation.

In **Fig. 3**, we show the results of an *in-situ* HRTEM study on elongated Au NPs embedded in SiO_2. **Fig. 3**(a-d) shows the time dependent HRTEM images revealing the shape evolution of one elongated Au NP, when the electron beam irradiation time is increased from 0 to 50 minutes. The shape change of the elongated Au NP with increase in irradiation time can be clearly seen. The variation of aspect ratio of Au NP with electron irradiation time is shown in **Fig. 4**. The aspect ratio of the Au NP showed a marked decrease from ~ 1.4 to 1 as the irradiation time is increased to 50 min. The observed shape recovery of elongated Au NP from ellipsoidal-to-spherical shape upon electron beam irradiation has an important significance because it offers a unique way to tailor down the aspect ratio of embedded NPs. The possible mechanisms underlying the observed electron-beam-induced shape evolution of elongated Au NPs embedded in silica matrix are discussed in the next section.

When an energetic electron beam penetrates a solid, electrons undergo elastic scattering with target nuclei and inelastic scattering with atomic electrons. The elastic collisions of incident electrons with target nuclei result in knock-on displacements of target atoms. The inelastic scattering of electrons leads to the excitation or ejection of atomic electrons. The possible mechanisms of atomic-electron excitation include ionization of core electrons, ionization of valence electrons leading to covalent bond breakage, elevation of valence electrons to exciton state and collective excitation of valence electrons into plasmons [**31**]. The energy deposited by electrons results in an increase in temperature of the irradiated area. The thermal energy deposited by electrons results in melting of small clusters and diffusion of constituent atoms in the irradiated area. This together with the atomic displacements caused due to elastic scattering of electrons can result in change in the size and shape of nanoparticles in the irradiated area. In addition, radiation enhanced atomic diffusion and stress relaxation in embedded NPs due to temperature rise of matrix can lead to change in their size and shape. Therefore, we estimate the temperature rise in the matrix and the atomic displacements caused by incident electrons. We have theoretically calculated the temperature rise (ΔT_e) in the SiO_2 matrix due to 200 keV electron beam irradiation using the formalism given by Liu and Rishbud [**21**]. The total energy loss (Q) of the electrons in the solid results in an increase in temperature (ΔT_e) of the matrix. The temperature rise of SiO_2 matrix due to electron beam irradiation for time t_e seconds is given by –

$$\Delta T_e = \frac{3JQ}{8ec_v Dd} R_e^2 \log\left(1+\frac{4Dt_e}{R_e^2}\right) ----(1)$$

where $D = k_t/c_v\, d$ (k_t is the thermal conductivity, c_v is specific heat and d is the density), J (=1.4x10^8 A/m^2) is the current density and R_e is the effective radius of the irradiated area. The rise in temperature (ΔT_e) of the SiO_2 matrix as a function of time (t_e) has been calculated using k_t = 130 J/m s K, d = 2200 Kg/m^3, c_v = 740 J/Kg K for the SiO_2 matrix. It has been observed that the temperature (ΔT_e) increases up to about 140^{o}C after electron beam irradiation for 50 minutes.

The maximum energy transferred to a nucleus of mass m_a by an electron of mass m_e and kinetic energy E is given by [**32**]-

$$E_{max} = \frac{2m_a E(E+2m_e c^2)}{[(m_a+m_e)^2 c^2 + 2m_a E]} ----(2)$$

For 200 keV electrons, E_{max} have been estimated to be 32.8 eV, 18.7 eV and 2.7 eV for O, Si and Au atoms, respectively. The estimated values of E_{max} for O and Si

atoms are higher than the corresponding displacement energies for O (9.3 eV) and Si (18.6 eV), reported for electron irradiation of SiO_2 films [**33**]. However, E_{max} for Au is much lower than the corresponding displacement energy of 25 eV. Therefore, 200 keV electron beam irradiation of SiO_2 matrix containing Au NPs results in knock-on displacements of O and Si atoms, but not that of Au atoms. The knock-on displacements of O and Si atoms can result in the relaxation of stress around the elongated Au NPs. It must be pointed out here that the cross sections for electron induced knock-on displacements of O and Si atoms are small. However, electron beam induced radiation enhanced diffusion (RED) of knock-on displaced O and Si atoms and temperature rise of silica have been shown to result in precipitation of Si nanocrystals in silica [**34**] and shape deformation of nanopores in silica [**34**]. The shape deformation of silica nanopores have been explained by electron beam induced softening of silica, which acts as a viscous fluid [**35**]. In the present case, elongated Au NPs in silica are fabricated by swift heavy ion irradiation and hence form during rapid quenching of transiently molten viscous fluid along ion track. Due to this they are not in a stable configuration because of the presence of interfacial stress. 200 keV electron beam irradiation leads to a temperature rise (140^{o}C) of silica together with radiation enhanced diffusion of knocked-on O and Si atoms in silica, which acts as a viscous fluid. We believe the cumulative effects of electron beam induced heating, softening of silica matrix and RED of knock-on displaced O and Si atoms result in relaxation of stress around Au NPs driving their ellipsoidal-to-spherical shape transition for energy minimization.

Conclusion

In summary, an *in-situ* HRTEM study of electron-beam-induced shape evolution of elongated Au NPs embedded in SiO_2 matrix has been performed. Electron beam irradiation results in decrease in aspect ratio of elongated Au NPs, which can be controlled by irradiation time. The theoretical calculations indicate that the electron-beam irradiation leads to temperature rise (140^{o}C) of silica matrix and knock-on displacements of O and Si atoms. The observed ellipsoidal-to-spherical shape transition of Au NPs embedded in silica can be ascribed to cumulative effects of electron beam induced heating, softening of silica matrix and RED of knock-on displaced O and Si atoms resulting in local stress relaxation.

Acknowledgements

SM is grateful to Department of Science and Technology, New Delhi for providing financial support under SERC Fast Track Young Scientist project.

Reference

1. Nie, S.; Emory, S.R. *Science* **1997**, *275*, 1102. **DOI**: 10.1126/science.275.5303.1102
2. Yin, Y.; Alivisatos, A. P. *Nature* **2005**, 437, 664. **DOI**: 10.1038/nature04165
3. Kano, H.; Kawata, S. *Opt. Lett.* **1996**, *21*, 1848. **DOI**: 10.1364/OL.21.001848
4. Beecroft, L. L. ; Ober, C. K. *Chem. Mater*. **1997**, *9*, 1302. **DOI**: 10.1021/cm960441a
5. Sanchez, E. J. ; Novotny, L. ; Xie, X. S. *Phys. Rev. Lett*. **1999**, *82*, 4014. **DOI**: 10.1103/PhysRevLett.82.4014
6. Gryczynski, I.; Malicka, J.; Shen, Y.; Gryczynski, Z.; Lakowicz, J. R. *J. Phys. Chem. B* **2002**, *106*, 2191. **DOI**: 10.1021/jp013013n
7. Stellacci, F.; Bauer, C. A.; Friedrichsen, T. M.; Wenseleers, W.; Marder, S. R.; Perry, J. W. *J. Am. Chem. Soc*. **2005**, *125*, 328. **DOI**: 10.1021/ja0281277
8. Jensen, T. R.; Malinsky, M. D.; Haynes, C. L.; and Duyne, R. P. Van *J. Phys. Chem. B* **2000**, 104, 10549. **DOI**: 10.1021/jp002435e
9. Kelly, K. L.; Coronado, E.; Zhao, L. L.; Schatz, G. C. *J. Phys. Chem. B* **2003**, *107*, 668. **DOI**: 10.1021/jp026731y
10. Schwartzberg, A. M.; Olson, T. Y.; Talley, C. E.; and Zhang, J. Z. *J. Phys. Chem. B* **2006**, *110*, 19935. **DOI**: 10.1021/jp062136a
11. Mishra, Y. K.; Mohapatra, S.; Kabiraj, D.; Mohanta, B.; Lalla, N. P.; Pivin, J. C.; Avasthi, D. K. *Scripta Mater.* **2007**, *56*, 629. **DOI**: 10.1016/j.scriptamat.2006.12.008
12. Mohapatra, S.; Mishra, Y. K.; Avasthi, D. K.; Kabiraj, D.; Ghatak, J.; and Varma, S. *J. Phys. D: Appl. Phys.* **2007**, *40*, 7063. **DOI**: 10.1088/0022-3727/40/22/030
13. Zheng, Y. B.; Huang, T. J.; Desai, A. Y.; Wang, S. J.; Tan, L. K.; Gao, H.; and Huan, A. C. H. *Appl. Phys. Lett.* **2007**, *90*, 183117. **DOI**: 10.1063/1.2736283
14. Mohapatra, S.; Mishra, Y.K.; Avasthi, D.K.; Kabiraj, D.; Ghatak, J.; Varma, S. *Appl. Phys. Lett.* **2008**, *92*, 103105. **DOI**: 10.1063/1.2894187
15. Mishra, Y. K.; Avasthi, D. K.; Kulriya, P. K.; Singh, F.; Kabiraj, D.; Tripathi, A.; Pivin, J. C.; Bayer, I. S.; and Biswas, A. *Appl*. Phys. Lett. **2007**, *90*, 73110. **DOI**: 10.1063/1.2642824
16. Roorda, S.; Dillen, T. V.; Polman, A.; Graf, C.; Blaaderen, A. V. and Kooi, B. J.; *Adv. Mater*. **2004**, *16*, 235. **DOI**: 10.1002/ADMA.200305742
17. Mishra, Y. K.; Singh, F; Avasthi, D. K.; Pivin, J. C.; Malinovska, D.; Pippel, E. *Appl. Phys. Lett.* **2007**, *91*, 063103. **DOI**: 10.1063/1.2764556
18. Awazu, K.; Wang, X.; Fujimaki, M.; Tominaga, J.; Aiba, H.; and Ohki, Y.; Komatsubara, T. *Phys.Rev. B* **2008**, 78, 054102. **DOI**: 10.1103/PhysRevB.78.054102
19. Dawi, E.A.; Rizza, G.; Mink, M.P.; Vredenberg, A.M.; Habraken, F.H.P.M. *J. Appl. Phys*. **2009**, *105*, 074305. **DOI**: 10.1063/1.3103267
20. Avasthi, D.K.; Mishra, Y.K.; Singh, F.; Stoquert, J.P. *Nucl. Instr. Meth. B* **2010**, *268*, 3027. DOI:10.1016/j.nimb.2010.05.033
21. Liu, Li-Chi; Rishbud, Subhash H. *J. Appl. Phys.* **1994**, *76*, 4576. **DOI**: 10.1063/1.357291
22. Yokota, Takeshi; Murayama, M.; Howe, J. M. *Phys. Rev. Lett.* **2003**, 91, 265504. **DOI**: 10.1103/PhysRevLett.91.265504
23. Bogle, K.A.; Dhole, S.D.; and Bhoraskar, V.N. *Appl. Phys. Lett.* **2006**, 88, 263105. **DOI**: 10.1063/1.2217712
24. Mahapatra, S.K.; Bogle, K.A.; Dhole, S.D.; and Bhoraskar, V.N. *Nanotechnology* **2007**, *18*, 135602. **DOI**: 10.1088/0957-4484/18/13/135602
25. Guzman, S. S.; Villarreal, N. E.; Ferrer, D.; Castro, A. T.; Gao, X; Zhou, J. P. and Yacaman, M. J. *Nanotechnology* **2007**, *187*, 335604. **DOI**: 10.1088/0957-4484/18/33/335604
26. Mishra, Y.K.; Mohapatra, S.; Avasthi, D.K.; Lalla, N.P.; Gupta, Ajay *Adv. Mat. Lett.* **2010**,1, 151. **DOI**: 10.5185/amlett.2010.4116
27. Ziegler, J. F.; Biersack, Z. P.; and Littmark, U. *The Stopping and Range of Ions in Solids* (Pergamon, New York **1985**).
28. Toulemonde, M.; Costantini, J. M.; Dufour, Ch.; Meftah, A.; Paumier, E.; and Studer, F. *Nucl. Instrum. Methods Phys. Res. B* **1996**, *116*, 37. **DOI**: 10.1016/0168-583X(96)00007-9
29. Brongersma, M. L.; Snoeks, E.; and Polman, A. *Appl. Phys. Lett*. **1997**, *71*, 1628. **DOI**: 10.1063/1.119999
30. Trinkaus, H.; and A. I. Ryazanov, *Phys. Rev. Lett.* **1995**, *74*, 5072. **DOI**: 10.1103/PhysRevLett.74.5072
31. Hobbs, L. W. *Introduction to Analytical Electron Microscopy* (Plenum, New York, **1979**), pp. *437–480*.
32. Balanzat, E.; and Bouffard, S. *Solid State Phenom.* **1993**, *30-31*, 7.

DOI: 10.4028/www.scientific.net/SSP.30-31.7
33. Pfeffer, R. L. *J. Appl. Phys*. **1985**, *57*, 5176.
DOI: 10.1063/1.335252
34. Du, Xi-wen; Takeguchi Masaki; Tanaka, Miyako; Pivin, Furuya, Kazuo *Appl. Phys. Lett*. **2003**, *82*, 1108.
DOI: 10.1063/1.1555691
35. Storm, A.J.; Chen, J.H.; Ling, X.S; Zandbergen, H.W.; Dekker, C. *J. Appl. Phys*. **2005**, *98*, 014307.
DOI: 10.1063/1.1947391

